Wavelet analysis for relating soil amplification and liquefaction effects with seismic performance of precast structures

Eleni Smyrou[1],*,†, İhsan Engin Bal[1], Panagiota Tasiopoulou[2] and George Gazetas[2]

[1]*Istanbul Technical University, Turkey*
[2]*National Technical University of Athens, Greece*

1. INTRODUCTION

Mainly for reasons of economy and speed of construction, precast concrete structures are preferred for industrial facilities, warehouses, car parks, etc. where large spans are required. Such structures, typically of low height and repeated geometry, consist of consecutive frames composed of individual columns and long-span rectangular or tapered beams, both ends of which are on pinned supports. The latter comprise one or two anchorage dowels, permitting rotation but preventing lateral movement. The frames are spanned with reinforced concrete planks bolted on the beam flanges with semi-rigid connections. The non-moment-resisting beam-column connections are the reason for their longer fundamental period, compared to that of a structure with monolithic connections, and for the limited redundancy of the structure.

During recent earthquakes, such as Kocaeli [1, 2], Emilia-Romagna [3, 4] and Christchurch [5, 6], precast buildings have suffered severe structural damage, mostly concentrated in the connection system, leading occasionally to collapse. Industrial buildings occupy large areas; thus they are mostly located in flat fields, founded on shallow isolated footings. Although, no specific geotechnical site investigation was conducted below the above reported damaged buildings, the site conditions in the vicinity of industrial and rural environments were described by soft soil layers, with high ground water table levels, while in several areas occurrence of liquefaction was reported. One could thus reasonably attribute part of the inflicted structural damage to soil effects in view of the long fundamental periods of such buildings (in the range of 0.5 to 2 s). Soil-amplified motions could be very rich in this period range. Soil non-linearity and liquefaction may enhance the importance of this period range. Several works have already underlined the significant influence of amplified spectral accelerations for large periods on the response of precast buildings [7–10]. Youd and Carter [11] showed that ground motion records on top of a soil layer that had liquefied exhibited a hump at long periods that may encompass the dominant periods of bridges.

During strong seismic excitation soil softening leads to lengthening of the fundamental period of the site and hence to substantial spectral accelerations at periods above 1 s [11–15]. By contrast, spectral accelerations at shorter periods tend to decrease (soil 'filtering'). With liquefaction-affected ground motions in particular, peak spectral values not only shift to even longer periods, but also can be significantly amplified despite the fact that peak ground accelerations are generally cut-off because of loss of soil strength. This spectral amplification, usually shown in the form of bulges around periods exceeding 2 s, is attributed to ground oscillation on top of the liquefied layers which continue beyond the strong shaking, accompanied by acceleration spikes because of sudden drop of excess pore pressure or dilatant response [14, 16].

---

*Correspondence to: Eleni Smyrou, Istanbul Technical University, Turkey.
†E-mail: esmyrou@itu.edu.tr

The main goal of the paper is to investigate the impact of such soil effects on the performance of typical precast structures. To this end, the precast case-study structures are subjected to 54 ground motions recorded on a variety of soils (hard, soft and liquefied soils) during 12 seismic events. Only level-ground records are considered in this paper, and no foundation-related failures because of liquefaction are within the scope of our work. Instead of the conventional examination of Fourier spectra, the estimation of soil effects, as imprinted on the recorded ground motions, is conducted using a wavelet-based method, which can provide information on the variable frequency and intensity content of the motion in time domain. Wavelet-based analysis is thus a useful tool in detecting if and when a certain acceleration record has been affected by soil softening, and most importantly if signs of liquefaction can be revealed, even if there is no clear evidence on the ground surface (e.g. sand boils, ground fissures and large settlement in the vicinity of the recording station).

2. EVALUATION OF SITE RESPONSE USING WAVELET-BASED ANALYSIS

Wavelet transform has gained ground in the analysis of signals with abrupt changes [17] such as earthquake ground motions [18–24]. Haigh et al. [25], for instance, show that the harmonic wavelet analysis is a versatile tool that can give information especially for occurrence of liquefaction, even if traditional time or frequency domain analysis is not available. Tezcan et al. [26] show the advantage of a wavelet-based approach over its Fourier-based counterpart, where time domain information is lost. Their study concludes that the energy localization patterns observed in the wavelet spectra from different sites and events can be used to detect nonlinear effects and characterize soil damping. Kramer et al. [27] present a set of wavelets and come to the conclusion that there is a sudden drop of available frequencies after a certain time step. Rezai and Ventura [28] work on the applicability of wavelet transform for the analysis of strong and weak ground motions recorded on rock of the Yerba Buena Island and on dredged sandfill in the nearby (about 2 km away) Treasure Island during the 1989 Loma Prieta earthquake. The major important feature of this data set is that liquefaction did occur in Treasure Island during strong shaking. Results of the application show that there are some large peaks at the highest resolution in the wavelet transforms, which can be attributed to a progressive change in the stiffness characteristics of the soil.

Wavelets are ideal to identify any phases of a signal with different frequency content and with localized time distribution. As Rezai and Ventura [28] concisely describe, wavelet transform represents a time-domain function as a linear combination of a family of basis functions that are generated by scaling (dilating or contracting) and shifting of a single function called mother wavelet. Mother wavelets are oscillatory with amplitudes that quickly decay to zero in both directions. Each scaled wavelet can be viewed as a bandpass filter with a particular frequency bandwidth and a center frequency. Appropriate discretization of the wavelet dilating and shifting parameters allows the wavelet series to cover all frequencies of interest and thus, represent any arbitrary signal (the ground motion in particular), as the exact sum of basis functions of finite length weighted by the wavelet components [28]. Thus, the time information is retained with a certain resolution in contradistinction to the conventional Fourier analysis that misses the apparent localization in time and frequency.

The effects of liquefaction on the frequency content of the recorded motions have been known for long: as shear waves propagate from bedrock the soil tends to de-amplify the low-period components of motion and to amplify the high-period components. It behaves as a filter that cuts off the high frequency components, while lengthening the duration of motion cycles [11]. Time domain is of key importance in liquefaction analyses, simply because excess pore pressure builds up as a function of time, resulting in progressive soil softening until liquefaction actually occurs. Although there is no distinct point before and after liquefaction, some insight can be obtained with the help of wavelet analysis. In contrast to Fourier transformation, which by definition cannot capture information in the time domain, wavelet analysis attains certain features of the ground motion by utilizing energy localization patterns.

So wavelet analysis is a powerful tool to associate characteristics of the recorded ground motion with the occurrence of soil softening in general, and liquefaction in particular. Wavelet analysis,

despite a similarity with Fourier analysis, differs from it in two main points: (i) the series can be expressed in any wave format, and (ii) the presence of waves is recorded in time domain. Given the predetermined locations in the time domain and scales, wavelet transform practically measures the similarity between the record and the scaled/shifted wavelet, through their inner product, over this predefined time-scale grid.

It should be mentioned, herein, that the detection of liquefaction in a record by means of wavelet procedure can be extremely useful because decision-making can be rendered automatic (i.e. by a computer) within a loss estimation framework. In the rapidly developing research in loss estimation, the information gathered during an earthquake event through an accelerograph network can be correlated to estimated losses as long as a definition of liquefaction is possible via accelerometer output. There are acceleration time history-based procedures to define whether liquefaction occurred or not [29–31], but these procedures do not provide information about the evolution of dominant frequency in time. A method to associate liquefaction with losses was proposed by Bird et al. [32], encouraging the inclusion of liquefaction phenomena in urban-level loss estimation studies that could be incorporated in decision making in the immediate aftermath of a catastrophe.

3. WAVELET ANALYSIS OF REAL ACCELEROGRAMS

The wavelet analyses presented here have been conducted using Matlab software and employing the Morlet wavelet [33]. From the several wavelets in the literature, the Morlet wavelet shown in Figure 1 is the most compatible with earthquake motions. It contains five cycles, with a shape quite similar to a ground motion record. **F1**

The maximum period of interest in the results depicted in the scalograms are limited to 4-s period. In the graphs given, the abscissa represents the real time, and the colors convey the match of the record at the relevant time slice with the pre-defined wavelet, or else the energy content, which is proportional to the level of amplification in terms of spectral acceleration. The energy content is produced as the multiplication of the amplitude and the frequency of the wavelet pieces summed up at each time step. The scalograms thus depict the fraction of the overall energy content (i.e. acceleration multiplied with time) of the record both in the time and frequency (period) domain. The wavelet analysis results are demonstrated for the acceleration records listed in Table I. Note that wavelet **T1** analysis was performed for several records among the ones listed in Table II and the results obtained **T2** consistently supported the findings explained below, which were deemed as the most eloquent and thus presented in detail. The PGA values of the records range between 0.21 and 1.43 g. The records have been categorized according to the soil conditions: (i) liquefied site, (ii) soft soil site without liquefaction and (iii) hard soil site. In the present study, soft soil sites are characterized those falling
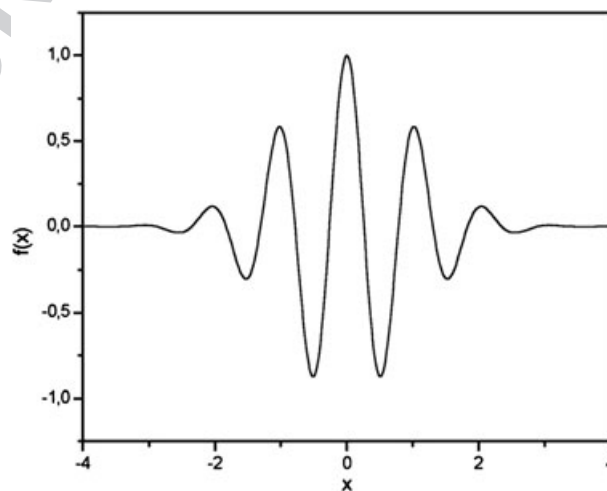

Figure 1. Morlet-type wavelet used in the analyses.

Table I. Acceleration records used for demonstration of wavelet analysis.

Event	Station	Site class	PGA (g)	Liquefaction
Kobe, Japan, 1995, M = 6.9	JMA	Hard soil	0.82	No
Chi Chi Earthquake, 1999, M = 7.6	TCU068	Soft soil	0.50	No
Superstition Hills, 1987, M = 6.5	Wildlife	Soft soil	0.21	Yes
Christchurch, 2011, M_L = 6.3	CBGS	Soft soil	0.64	Yes
	CCCC	Soft soil	0.41	Yes
	HVSC	Hard soil	1.43	No

into class D or E, according to NEHRP soil classification system, or C and D according to EC8, with shear wave velocity, V_{s30}, less than 350 m/s.

To develop insight into how liquefaction affects the ground response in real time, Wildlife Site record from Superstition Hills 1987 Earthquake was chosen as a characteristic unambiguous case of liquefaction, given the fact that the excess pore water pressures were recorded on site at various depths during shaking. The wavelet map is shown in Figure 2 along with the acceleration and excess pore water pressure ratio time-histories, after Dobry et al. [12]. The ground response can be approximately divided in three time phases: (i) 0–13 s: the intensity of the shaking is still low and excess pore water pressures hardly developed, (ii) 13–22 s: the ground shaking intensified and excess pore water pressure gradually increased, indicating soil softening and (iii) 22 s to the end: excess water pressures slowly reached a plateau and liquefaction (r_u = 1) occurred close to the surface (transducer P5), resulting in long-period oscillation of the overlying clayey layer after the end of strong shaking, with acceleration spikes indicative of soil dilatancy.

During the first time interval, the wavelet map does not show any dominant periods, while the energy content is so low that the period contours cannot be distinguished. In the second interval, the wavelet map explicitly demonstrates how the period content of the motion gradually increases from 0.5 to 2 s as excess pore water pressures develop. Thus, wavelet analysis is able to capture in real time the well-known mechanism of period elongation because of soil softening. The colors of the contours confirm that the strong part of shaking corresponds to this time frame (13−22 s). Finally, during the last interval, beyond 22 s, as liquefaction slowly occurs, the period content now takes values between 3 and 4 s, as shown by the light blue bulbs. Moreover, the energy content diminishes only slightly because of liquefaction-induced oscillation of the soil 'crust' layer accompanied with acceleration spikes. It is evident that, translating the contours of the wavelet map into spectral accelerations, amplification of the latter is expected in a period range from 1 to 2.5 s because of significant soil softening and 2.5 to 4 s because of liquefaction, in agreement with Youd and Carter [11].

Two more typical cases of liquefaction-affected free-field records, CCCC and CBGS, from the Christchurch M_w = 6.3 Earthquake (February 2011) are examined (Figures 3 and 4 respectively). Note that the soil in both aforementioned stations, composed of alluvial sand, had demonstrably liquefied, as manifested by sand boils on the ground surface [34]. The scalograms in Figures 3 and 4 unveil a repetitive pattern, similar to the Wildlife record: before liquefaction, while pore water pressures were rising (transition phase), the energy is concentrated in a period range around 1 s, a combination of the dominant periods of the motion itself and of the typical period of soft soil sites. After liquefaction energy concentration appears in higher period values, 3–4 s, indicating severe soil softening.

Overall, the common characteristic in all the above wavelet maps of liquefaction-affected motions is the gradual period lengthening to 1 to 2 s and the formation of secondary pulses with periods in the range of 2–4 s. In order to determine whether this pattern applies only to liquefied sites, wavelet analysis is performed for soft (without liquefaction) and hard soil sites. Thus, a record from hard soil site without any trace of excess pore water pressure development, let alone liquefaction, in a very intense ground motion case, such as the JMA record in 1995 Kobe had been examined. Note that the energy content shows a concentration at periods of about 1 s, or slightly higher, early in the shaking. Later on, the energy concentrates at lower periods, contrary to what was noted in Figures 3

Table II. The acceleration records used in the structural analyses.

Event	Station	Site class	PGA (g)	Liquefaction
Kobe	JMA	Hard soil	0.82	No
	Kakogawa	Hard soil	0.25	No
	Nishi-Akashi	Hard soil	0.51	No
	Port Island	Soft soil	0.23	Yes
	Takatori 00	Soft soil	0.61	Yes
	Takatori 90	Soft soil	0.62	Yes
	Amagasaki	Soft soil	0.30	No
Kocaeli	Sakarya	Hard soil	0.33	No
Landers	Joshua	Soft soil	0.31	No
Niigata	Kawagishi	Soft soil	0.23	Yes
Superstition Hills	Wildlife	Soft soil	0.21	Yes
San Fernando	PUL	Hard soil	1.49	No
Chi-chi 1999	TCU068	Soft soil	0.57	No
	CHY028	Soft soil	0.69	No
Loma Prieta	LPG	Soft soil	0.63	No
Northridge	WPI	Soft soil	0.28	No
ChCh Feb 2011	CBGS	Soft soil	0.64	Yes
	CCCC	Soft soil	0.41	Yes
	CHHC	Soft soil	0.36	Yes
	CMHS	Soft soil	0.37	Yes
	HPSC	Soft soil	0.23	Yes
	HVSC	Hard soil	1.43	No
	LPCC	Hard soil	0.92	No
	PPHS	Soft soil	0.19	No
	PRPC	Soft soil	0.72	Yes
	REHS	Soft soil	0.72	Yes
	RHSC	Soft soil	0.30	No
	SHLC	Soft soil	0.32	Yes
	SMTC	Soft soil	0.18	No
Darfield Sept 2010	CBGS	Soft soil	0.15	No
	CCCC	Soft soil	0.18	No
	CHHC	Soft soil	0.15	No
	CMHS	Soft soil	0.25	No
	HPSC	Soft soil	0.11	Yes
	HVSC	Hard soil	0.66	No
	LPCC	Hard soil	0.24	No
	PPHS	Soft soil	0.18	No
	PRPC	Soft soil	0.20	Yes
	REHS	Soft soil	0.24	No
	RHSC	Soft soil	0.18	No
	SHLC	Soft soil	0.18	No
	SMTC	Soft soil	0.16	Yes
ChCh 2011 June	CBGS	Soft soil	0.15	No
	CHHC	Soft soil	0.19	No
	CMHS	Soft soil	0.19	No
	HPSC	Soft soil	0.16	Yes
	HVSC	Hard soil	0.66	No
	LPCC	Hard soil	0.54	No
	PPHS	Soft soil	0.13	No
	PRPC	Soft soil	0.34	No
	REHS	Soft soil	0.24	No
	RHSC	Soft soil	0.19	No
	SHLC	Soft soil	0.16	No
	SMTC	Soft soil	0.08	No

and 4 in the liquefaction cases. Evidently, the particular dominant periods and their evolution in time reflect mostly the fault rupture mechanism and (recognized) 'directivity' effects (Figure 5). **F5**

Usually soft-soil records convey a period content below 2 s [35]. Exceptions abound however, even without the occurrence of liquefaction. Such records have been affected either by extreme
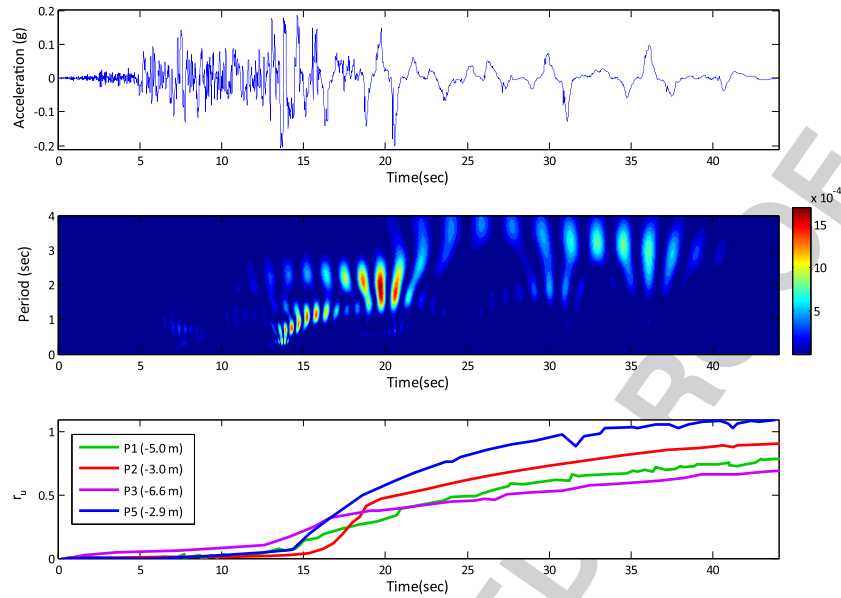
Figure 2. Ground acceleration, wavelet map and excess pore pressure ratios at various depths versus time for the Superstition Hills, US (1987) Event—Wildlife recorder (NS) with observed liquefaction.

soil conditions (e.g. CDAO record in Mexico earthquake, 1985) or near-fault effects (directivity, fling-step etc.). The TCU068 record from Chi Chi 1999 earthquake, containing a fling-step pulse, is examined here via wavelet analysis. The wavelet map in Figure 6 reveals abrupt energy **F6** diffusion in a period range of 2–3 s, as soon as the fling pulse arrives at about 6 s. The pulse appears in the wavelet map like an eruption of energy with rich frequency content, followed by a slow decrease in the period range and values.

Last, a case of a very strong record on very hard soil (i.e. class B-C according to NEHRP): the HVSC record from Christchurch earthquake (Figure 7). Notice that the period content remains **F7** clearly around 0.5 s during strong shaking as expected [35].

In conclusion, wavelet analysis, when applied to large number or records, can identify characteristic patterns directly related to particular effects on ground motions, such as liquefaction, soil softening or even near-fault effects (though the last case was not thoroughly established in this work). This can be a huge advantage in categorizing ground motions, but it can also serve as an interpretation tool for observed structural performance.
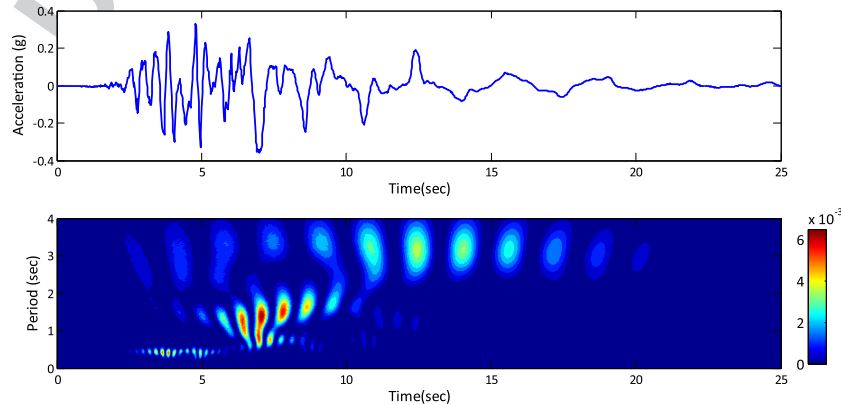
Figure 3. Time history and wavelet map for the Christchurch, New Zealand (2011) Event—CCCC recorder (EW) with observed liquefaction.
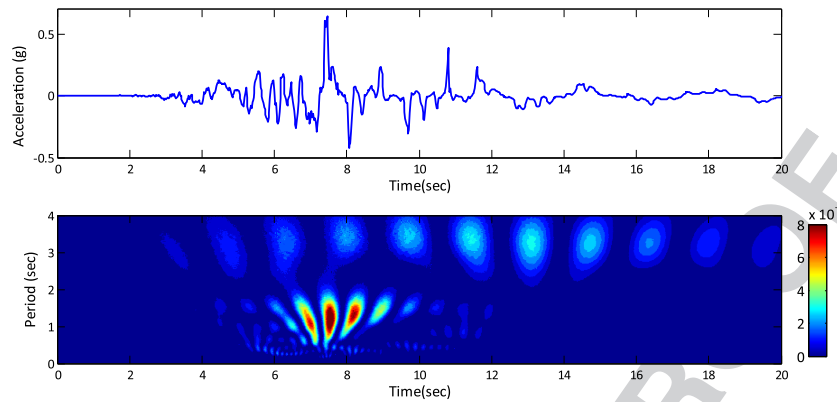
Figure 4. Time history and wavelet map for the Christchurch, New Zealand (2011) Event—CBGS recorder (S54W) with observed liquefaction.

4. SELECTION OF GROUND MOTION RECORDS

The ground motion records, used for the dynamic analysis of precast structures in the following, are selected from 12 different seismic events on both soft and hard soil sites, as shown in Table II. The distinction between hard and soft soil cases was made based on the reported soil properties of the recorders in the NGA Ground Motion PEER Database. Fifty four records are used in total, seventeen of which exhibited liquefaction according to literature references or/and field evidence when available, affirmed with wavelet analyses run for randomly selected records. The selected ground motions cover a wide period range of spectral accelerations, reflecting the intensity of the seismic event and the soil effects. Emphasis is given on records on soft soil sites, which are expected to mostly affect the precast structures because of concurrence of dominant period content.

5. EXAMINED CASE STUDIES AND NUMERICAL MODELING

Three case studies have been examined in this work, all from the same industrial facility located in Istanbul, an area seismically affected by the North Anatolian Fault. Although limited in number, the case studies considered are representative of RC precast structures in terms of structural system and construction details. The structural details of the facility in question are slightly modified because of confidentiality issues. The structure consists of two separate units: (i) the main production hall and storage, and (ii) the loading ramp (Figure 8). The loading   **F8**
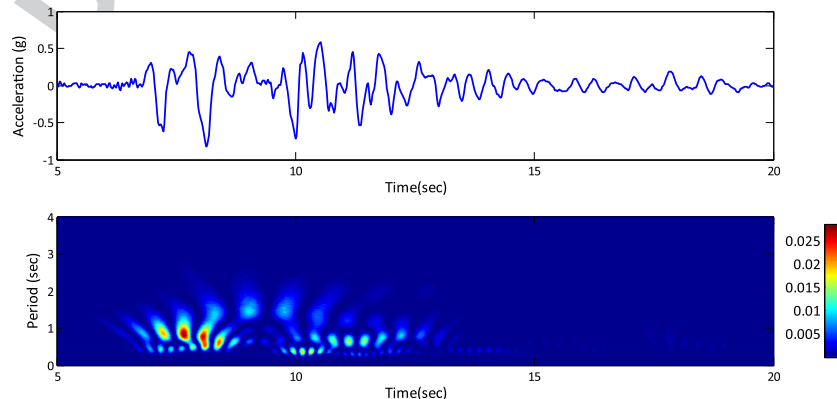

Figure 5. Time history and wavelet map for Kobe Earthquake (1995)—JMA recorder (NS) on hard soil site with no liquefaction.
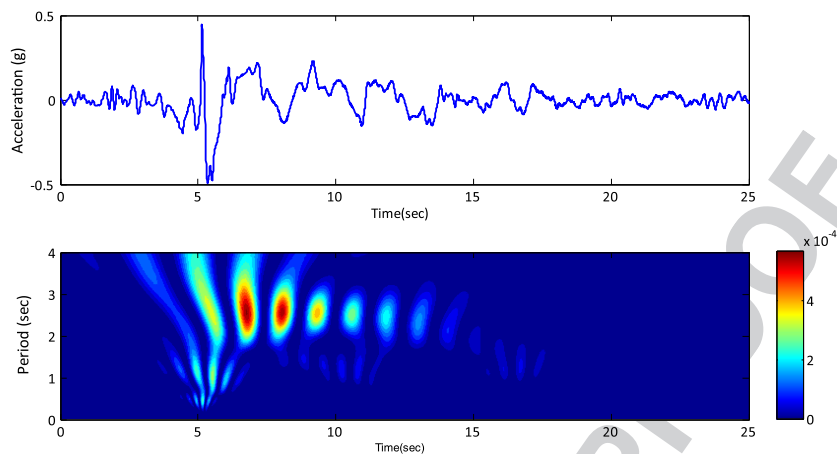
Figure 6. Time history and wavelet map for near-fault TCU068 recorder (EW) on soft soil site during Chi Chi Earthquake (1999).

ramp consists of two types of frames, the only difference of which is the height of the first floor. The frames, running in one direction and placed in every 10 m, constitute the bearing system. There is no beam between the frames in the transverse direction, as often met in construction practice in most European countries. The roof consists of double tee plates that are fixed to the beams, a property that allows a rigid diaphragm behavior. C35 concrete and S220 reinforcing steel are the characteristic values indicated in the design and were used for modeling. The beams simply sit on the columns. The beam-column connection is provided by means of two bars acting as anchorage dowels, which allow rotation but prevent lateral movement creating a connection that is not moment resisting and therefore modeled as a pinned one. Details of similar connections and their response to seismic actions can be found in [36].

In summary, the facility examined comprises three different types of frames: (i) the single-story frame of the main production hall (Case Study 1), (ii) the two-story frame of the loading ramp (Case Study 2a) and (iii) the two-story taller frame of the loading ramp (Case Study 2b). Once modeled with distributed plasticity elements, the three structures exhibit fundamental periods of 1.0, 1.22 and 1.38 s, respectively.

The frames have been modeled in OpenSees. A representative middle frame has been extracted from each structure applying the load and mass from its tributary area. Concrete02 [37] and Steel02 [38] cyclic uniaxial material models have been employed for modeling reinforced concrete. The connection of the columns to the beams has been modeled by using perfect flexural
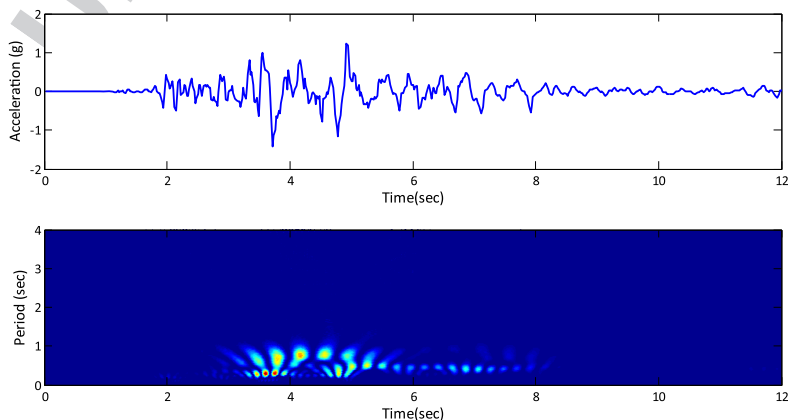

Figure 7. Time history and wavelet map for the Christchurch, New Zealand (2011) Event—HVSC recorder (S26W) on hard soil site.
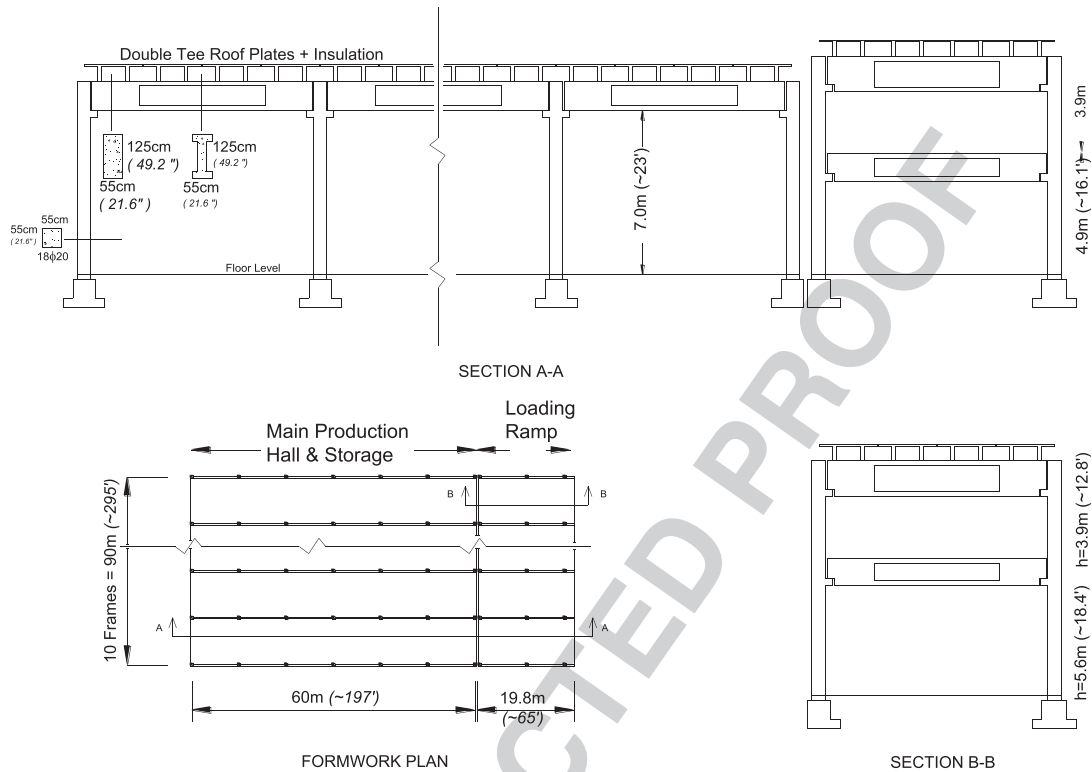
Figure 8. Formwork plan and sections of the industrial facility examined.

hinges. Because of the connection of the roof double tee plates to the beams, the rigid diaphragm assumption is valid.

Whereas the actual factory has frames founded on isolated footings, in order to be consistent with the soft/liquefied soil records utilized herein, it is assumed that in such soil the foundation should contain piles, a cost-prohibitive solution though, which will effectively fix the supports of the frames. As already mentioned kinematic distress of such foundations because of soil lateral displacements following liquefaction ('lateral-spreading') are not considered. It is only the effects of level-ground motions with their liquefaction-inflicted long-period humps that are analyzed in this paper.

6. SEISMIC PERFORMANCE OF PRECAST STRUCTURES

Proceeding in the seismic analysis of precast structures of fundamental periods between 1 and 1.4 s and based on the wavelet analysis findings, it is expected that the structural performance will be predominantly affected by records on liquefied sites and secondarily by soft soil sites, taking also into account possible period elongation of the structure because of nonlinear behavior. In order to obtain a better insight into the individual structural response, a simple comparison is presented initially in Figures 9 and 10, where Case Study Structure 1 (T = 1.0 s) **F9 F10** is subjected to two records from the Kobe 1995 earthquake, the Amagasaki and the Port Island records. The former had only a minor influence from excess pore water pressures near the end of shaking and is thus considered to be a typical of soft soil site with a period range below 2 s. The latter is identified with liquefaction after about 8 s of shaking, at least partial, because of high permeability of reclaimed soils and consequent rapid drainage [13].

It should be noted that the spectral acceleration demand for T = 1.0 s from the Amagasaki record is nearly equal to that of the Port Island Record (0.9 g). This value corresponds to the mobilization of the moment capacity of the columns, and is therefore an upper bound. Considerably higher displacement
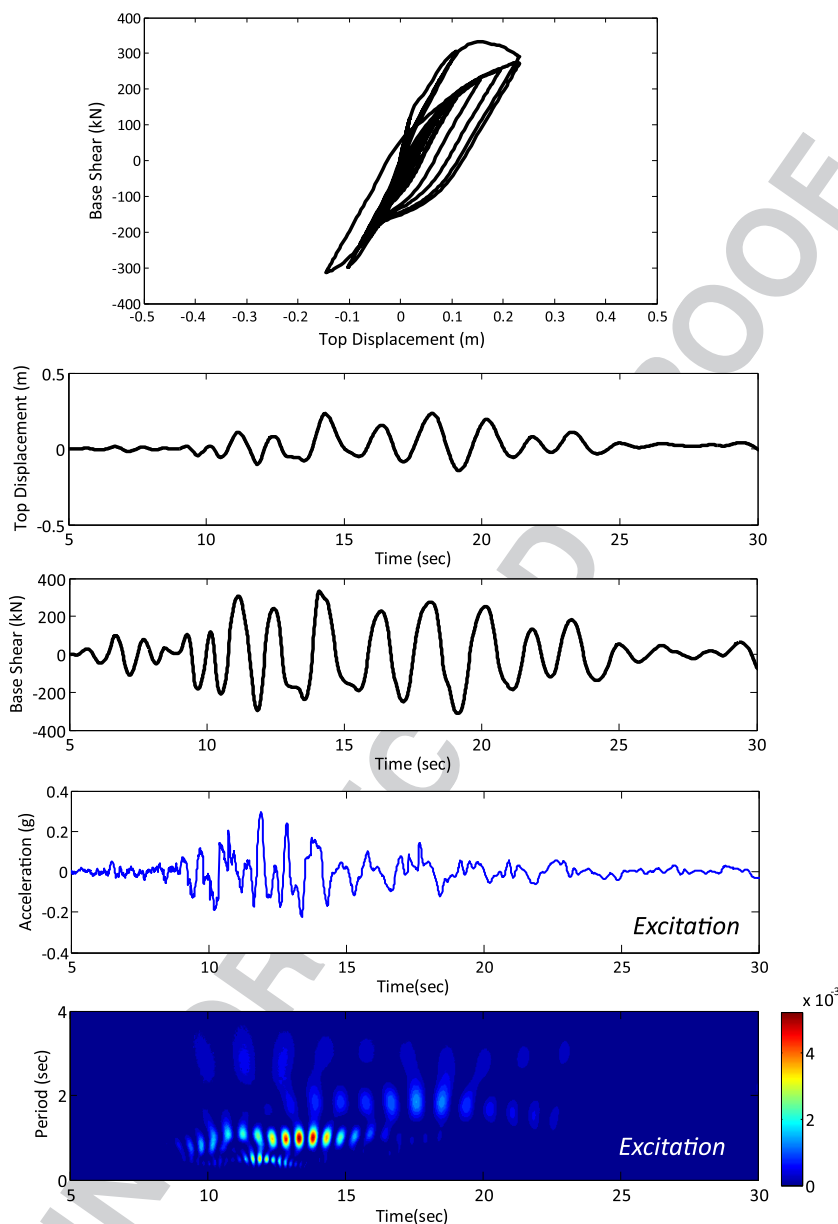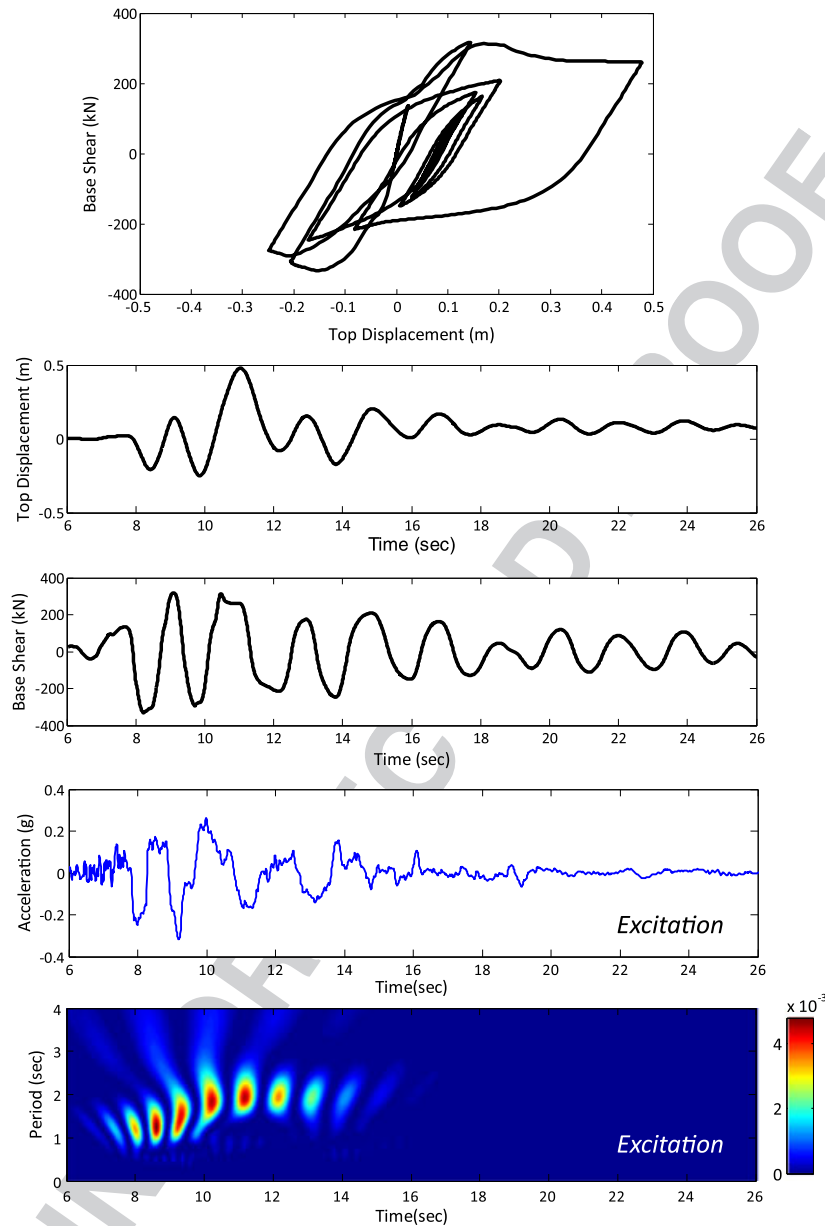
Figure 9. Base shear and top displacement response of Case Study 1 for the Kobe Event, Amagasaki Record w/o liquefaction $(Sa(T_1) = 0.9\,g)$.

(48 cm) is obtained for the Port Island record with liquefaction; the corresponding hysteretic loop area, indicative of the demand introduced in the structure, is also larger. Maximum displacement attained in the Amagasaki record with the Port Island record parameter is only 22 cm. This mere observation helps in answering the very question of this study: do the liquefaction-affected ground motions have more damage potential for precast structures even if the elastic spectral demand of the records with liquefaction are equal to or less than that of the soft soil records without liquefaction?

Zooming in on the plots of Figures 9 and 10, 10 distinct cycles between 8 and 26 s in the displacement time-histories can be distinguished in both records. Despite the equal number of cycles, the average displacement of these peaks is 12.5 cm with Amagasaki while the same quantity is 17.0 cm with Port Island record. Although hard to generalize, this finding indicates that the displacement demand itself is the critical parameter in determining the response of the structure, at least for the cases mentioned here.

Figure 10. Base shear and top displacement response of Case Study 1 for the Kobe Event, Port Island Record w/ liquefaction ($Sa(T_1) = 0.9\,g$).

The results of all the nonlinear time-history analyses conducted are presented in terms of the spectral acceleration value at the fundamental period of the structure, $Sa(T_1)$, is utilized. In order to better represent the damage on the structure, the widely used damage index of Park and Ang [39] has been employed (Equation 1).

$$D = \frac{\delta_M}{\delta_u} + \frac{\beta}{Q_y\delta_u}\int dE \qquad (1)$$

where δ_M is the deformation under earthquake, δ_u is the ultimate deformation under monotonic loading found by first mode pushover analysis in this study, Q_y is the calculated yield strength (if the maximum strength, Q_u, is smaller than Q_y, Q_y is replaced by Q_u), dE is the incremental absorbed hysteretic energy and β is suggested as 0.15 [39].

In Figures 11–13 the comparison between the Park & Ang damage index and the Sa(T1) values is illustrated. A value of Park & Ang index less or equal than 0.4 can be interpreted as repairable damage, from 0.4 to less than 1.0 as non-repairable damage, and larger than 1.0 as failure [39]. There is a distinction between hard (low non-linear effects), soft (high non-linear effects) and liquefied soil sites. For the Main Production Hall of the facility (Case Study 1–1.0 s fundamental period), 23 out of the 53 records proved to be destructive leading to its collapse. Twelve of these critical records have traces of liquefaction. Interestingly, the results indicate that records with higher $Sa(T_1)$ produce less damage than the records with liquefaction, but with lower $Sa(T_1)$. It is noted that the Park & Ang damage index considers both the maximum nonlinear displacement and the hysteretic energy; thus, the effect of number (or else duration of motion) and amplitude of cycles is inherently incorporated in the results presented in Figures 11–13. It would have been interesting to be able to discern between the effects of liquefaction and duration of motion. In other words, is the main cause of damage because of liquefaction-induced soil softening (period elongation) or because of liquefaction-induced duration lengthening? Although, clearly, both effects may contribute, there is no way to distinguish which is dominant. But in any case both are the consequence of liquefaction, and this is a main thesis of the paper.

What is quite clear in Figures 11 and 13 is that the records with clear liquefaction traces inflict higher damage on average. Bearing in mind that spectral acceleration demand is a particularly important parameter in code design, it is interesting to notice that the red dots (i.e. the damage caused by liquefaction records) cause the highest damage at low spectral acceleration demands.

Another observation derived from Figures 11 and 13 is that the hard soil records consistently induce much less damage than the soft soil and liquefaction records. The difference between soft and liquefaction records, on the other hand, is smaller but consistently indicating more damage with the liquefaction records, even for the same spectral acceleration demand. It can thus be safely deduced that liquefaction-affected level-ground motions systematically impose a greater threat to precast structures in terms of seismic demand even for low values of elastic spectral acceleration demand, even if other detrimental consequences of liquefaction such as foundation settlement and rotation, or lateral spreading, have been avoided.

Finally, note the extremely high damage indices (values > 3.5) corresponding to Port Island and Kawagishi records in Figures 12 and 13. Such values can be associated with the long-period motion characterizing the aforementioned records, which was not produced by liquefaction but originated by the source and the propagation path, and amplified by deep sediments of regional scale [40].
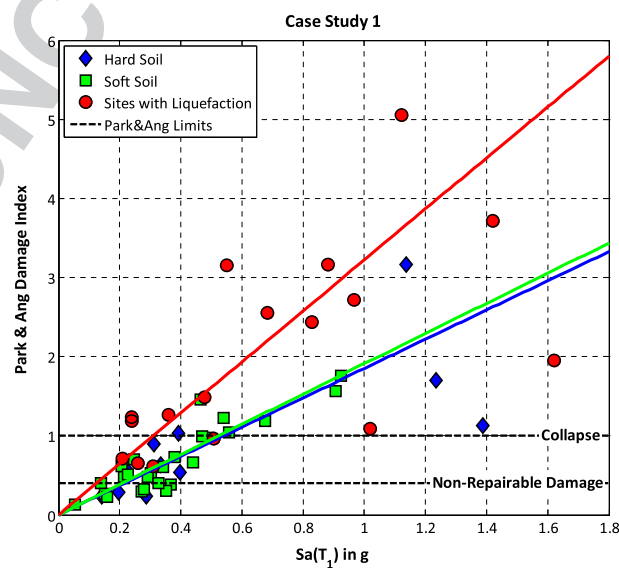

Figure 11. Comparison of the spectral acceleration values at the fundamental period for Case Study 1 with the Park & Ang damage index.
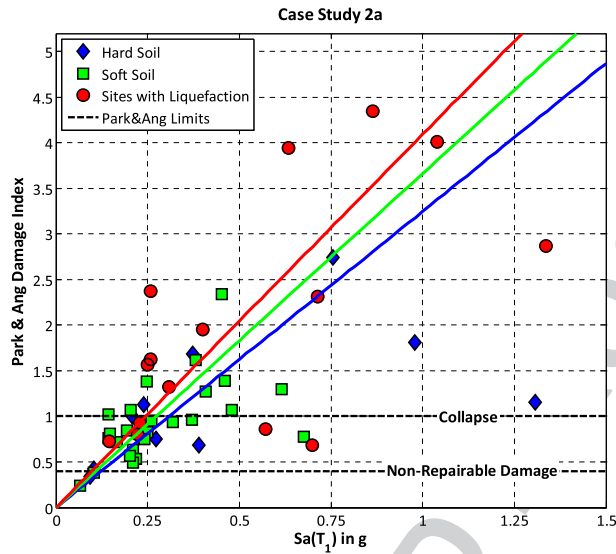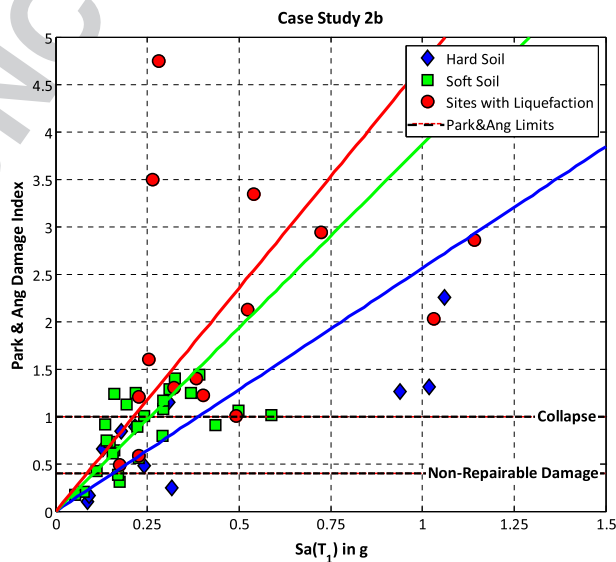
Figure 12. Comparison of the spectral acceleration values at the fundamental period for Case Study 2a with the Park & Ang damage index.

7. CONCLUSION

In this work, numerous nonlinear time-history analyses have been conducted of three structures, typical of precast-concrete industrial facilities, using numerous records from different seismic events as excitation. It was consistently demonstrated that, for such structures, records on level ground bearing the effect of liquefaction have stronger damage potential even for low values of elastic spectral acceleration demand. It was confirmed that elastic spectral acceleration is not a sufficient engineering demand parameter for design purposes, but the number of cycles and most importantly the amplitude of nonlinear displacements must be considered. Soil effects, imprinted on ground motions, should definitely be taken into account. For that purpose, a method based on wavelet analysis was introduced to detect the evolution of the energy and frequency content of the ground motion in time. A set of useful observations based on the period changes versus time has

Figure 13. Comparison of the spectral acceleration values at the fundamental period for Case Study 2b with the Park & Ang damage index.

been presented in order to identify the soil effects and categorize the ground motions into: (i) hard soil, (ii) soft soil and (iii) deeply liquefied soil. The results obtained make it possible to determine whether liquefaction occurred at site or not, the approximate time of onset of liquefaction, and, most importantly, the frequency content of the liquefaction-affected record.

REFERENCES

1. Saatcioglu M, Mitchell D, Tinawi R, Gardner NJ, Gillies AG, Ghobarah A, Anderson DL, Lau D. The August 17, 1999 Kocaeli (Turkey) earthquake-damage to structures. *Canadian Journal of Civil Engineering* 2001; **28**(8):715–773.
2. EERI. *Kocaeli, Turkey, Earthquake of August 17, 1999*. Earthquake Spectra supplement, 2000.   Q4
3. EPICentre Field Observation Report No. EPI-FO-200512 (2012), The 20th May 2012 Emilia Romagna Earthquake, [Available at http://www.ucl.ac.uk/~ucestor/research-earthquake/EPI Centre_Report_EPI-FO-200512.pdf].
4. Bournas DA, Negro P, Taucer FF. Performance of industrial buildings during the Emilia earthquakes in Northern Italy and recommendations for their strengthening. *Bulletin of Earthquake Engineering* 2014; **12**(5):2383–2404.
5. Fleischman RB, Restrepo JI, Pampanin S, Maffei JR, Seeber K, Zahn FA. Damage evaluations of precast concrete structures in the 2010–2011 Canterbury earthquake sequence. *Earthquake Spectra* 2014; **30**(1):277–306.
6. Tasiopoulou P., Smyrou E., Bal I.E., Gazetas G., Vintzileou El. (2011) Geotechnical and structural field observations from Christchurch, February 2011 Earthquake, in New Zealand, Research Report, NTUA, October 2011, website: http://geoengineer.org/files/ Tasiopoulou_et_al_2011.pdf
7. Baird A, Diaferia R, Palermo A, Pampanin S. Parametric investigation of seismic interaction between precast concrete cladding systems and moment resisting frames. *Structures Congress* 2011; **2011**:1286–1297.
8. Belleri A, Brunesi E, Nascimbene R, Pagani M, Riva P. Seismic performance of precast industrial facilities following major earthquakes in the Italian territory. *Journal of Performance of Constructed Facilities* 2014. DOI:10.1061/(ASCE)CF.1943–5509.0000617,04014135.
9. Magliulo G, Ercolino M, Manfredi G. Influence of cladding panels on the first period of one-story precast buildings. *Bulletin of Earthquake Engineering* 2015; **13**(5):1531–1555.
10. Magliulo G, Ercolino M, Petrone C, Coppola O, Manfredi G. Emilia earthquake: the seismic performance of precast RC buildings. *Earthquake Spectra* 2014; **30**(2):891–912.
11. Youd TL, Carter BL. Influence on soil softening and liquefaction on spectral acceleration. *ASCE Journal of Geotechnical and Geoenvironmental Engineering* 2005; **131**(7):811–825.
12. Dobry R, Elgamal AW, Baziar M, Vucetic M. Pore pressure and acceleration response of wildlife site during the 1987 earthquake. *Proc., 2nd U.S.–Japan Workshop on Liquefaction, Large Ground deformation and Their Effects on Lifelines*. National Center for Earthquake Engineering Research: Buffalo, N.Y., 1989. p 145–160.
13. Davis RO, Berrill JB. Energy dissipation and liquefaction at Port Island, Kobe. *Bulleting of New Zealand National Society for Earthquake Engineering*, **31**. : Waikanae, 1998. p 31–50.   Q5
14. Youd T, Steidl J, Nigbor R. Lessons learned and need for instrumented liquefaction sites. *Soil Dynamics and Earthquake Engineering* 2004; **24**(9–10):.   Q6
15. Youd, T. L. & Carter, B. (2003), Influence of soil softening and liquefaction on response spectra for bridge design, Report No. UT-03.07, University of Utah.
16. Elgamal, A.W., Dobry, R., Parra, E., and Yang, Z. (1998) Soil dilation and shear deformation during liquefaction, *Fourth International Conference on Case Histories in Geotechnical Engineering*, St Louis, Missouri, March 8–15, 1998, Prakash S. (ed.): 22   Q7
17. Newland DE. Random vibrations, spectral and wavelet analysis. *Longman Scientific and Technical* (3rd edn).. Harlow, Essex, England; and John Wiley: New York, 1993.
18. Basu B, Gupta VK. Seismic response of SDOF systems by wavelet modelling of nonstationary processes. *ASCE Journal of Engineering Mechanics* 1998; **124**(10):1142–1150.
19. Iyama J, Kuwamura H. Application of wavelets to analysis and simulation of earthquake motions. *Earthquake Engineering and Structural Dynamics* 1999; **28**(3):252–272.
20. Tai M, Fushimi M, Tatsumi Y, Irikura K. Separation of source and site effects using wavelet transform coefficients. *Proceedings of the 12th World Conference on Earthquake Engineering*Paper No. 2332. : Auckland, New Zealand, 2000.
21. Spanos PD, Giaralis A, Politis NP. Numerical treatment of seismic accelerograms and of inelastic seismic structural responses using harmonic wavelets. *Computer-Aided Civil and Infrastructure Engineering* 2007; **22**:254–264.
22. Spanos PD, Failla G. Evolutionary spectra estimation using wavelets. *Journal of Engineering Mechanics* 2004; **130**:952–960.
23. Garini E, Makris N, Gazetas G. Elastic and inelastic systems under near-fault seismic shaking: acceleration records versus optimally-fitted wavelets. *Bulletin of Earthquake Engineering* 2015; **13**:459–482.

24. Loli M, Anastasopoulos I, Knappett JA, Brown MJ. Use of Ricker wavelet ground motions as an alternative to push-over testing. *Proc. 8th Int. Conf. on Physical Modelling in Geotechnics 2014*14–17 January. : Perth, Australia, 2014. Q8
25. Haigh SK, Teymur B, Madabhushia SPG, Newlanda DE. Applications of wavelet analysis to the investigation of the dynamic behaviour of geotechnical structures. *Soil Dynamics and Earthquake Engineering* 2002; **22**:995–1005.
26. Tezcan J, Puri V, Cheng Q. Wavelet-based estimation of site response. *14th World Conference on Earthquake Engineering*. : Beijing, China, 2008. Q9
27. Kramer SL, Hartvigsen AJ, Sideras SS, Ozener PT.(2011) Site response modeling in liquefiable soils, *4th IASPEI/IAEE International Symposium*: *Effects of Surface Geology on Seismic Motion*, August 23–26.
28. Rezai M, Ventura CE. Analysis of strong and weak ground motions recorded at two sites during Loma Prieta earthquake by wavelet transform. *Canadian Journal of Civil Engineering* 2002; **29**:157–170.
29. Suzuki T, Shimizu Y, Nakayama W. Characteristics of strong motion records at the liquefied sites and judgment for liquefaction. *11th European Conference on Earthquake Engineering*. Paris, France, 1998. Q10
30. Takada S, Ozaki R. (1997) A judgment for liquefaction based on strong ground motion, *Proceedings of the 24th JSCE Earthquake Engineering Symposium*, Kobe, JSCE (in Japanese).
31. Rui S, Fuhui T, Longwei C. Blind detection of liquefaction by existing methods for New Zealand ML6.3 earthquake on Feb. 22, 2011. *Earthquake Engineering and Engineering Vibration* 2011; **10**:465–474.
32. Bird JF, Bommer JJ, Crowley H, Pinho R. Modelling liquefaction-induced building damage in earthquake loss estimation. *Soil Dynamics and Earthquake Engineering* 2006; **26**:15–30.
33. Goupillaud P, Grossman A, Morlet J. Cycle-octave and related transforms in seismic signal analysis. *Geoexploration* 1984; **23**:85–102.
34. Smyrou E, Tasiopoulou P, Bal IE, Gazetas G. Ground motions versus geotechnical and structural damage in the February 2011 Christchurch Earthquake. *Seismological Research Letters* 2011; **82**(6):882–892.
35. Seed HB. Evaluation of soil liquefaction effects on level ground during earthquakes. *Liquefaction Problems in Geotechnical Engineering*. American Society of Civil Engineers, Preprint 2752: N.York, 1976. p 1–104.
36. Psycharis NI, Mouzakis HP. Shear resistance of pinned connections of precast members to monotonic and cyclic loading. *Engineering Structures* 2012; **41**:413–427.
37. Yassin MHM. *Nonlinear Analysis of Prestressed Concrete Structures under Monotonic and Cycling Loads*. PhD dissertation, University of California: Berkeley, 1994.
38. Filippou FC, Popov EP, Bertero VV. Effects of bond deterioration on hysteretic behavior of reinforced concrete jointsReport EERC 83–19. *Earthquake Engineering Research Center*. University of California: Berkeley, 1983.
39. Park Y, Ang AH. Mechanistic seismic damage for model reinforced concrete. *ASCE Journal of Structural Engineering* 1985; **111**:722–73.
40. Kudo K., Uetake T, Kanno T. (2000) Re-evaluation of nonlinear site response during the 1964 Niigata earthquake using the strong motion records at Kawagishi-cho, Niigata city, *Proceedings of the 12th Word Conference in Earthquake Engineering*, Vancouver.

Author Query Form

Dear Author,

During the copyediting of your paper, the following queries arose. Please respond to these by annotating your proofs with the necessary changes/additions.

• If you intend to annotate your proof electronically, please refer to the E-annotation guidelines.

• If you intend to annotate your proof by means of hard-copy mark-up, please use the standard proofing marks. If manually writing corrections on your proof and returning it by fax, do not write too close to the edge of the paper. Please remember that illegible mark-ups may delay publication.

Whether you opt for hard-copy or electronic annotation of your proofs, we recommend that you provide additional clarification of answers to queries by entering your answers on the query sheet, in addition to the text mark-up.

Query No.	Query	Remark
Q1	AUTHOR: Please confirm that given names (red) and surnames/family names (green) have been identified correctly.	
Q2	AUTHOR: Please provide an abstract.	
Q3	AUTHOR: Figure 5 was not cited in the text. An attempt has been made to insert the figure into a relevant point in the text – please check that this is OK. If not, please provide clear guidance on where it should be cited in the text.	
Q4	AUTHOR: Please provide city location for reference 2.	
Q5	AUTHOR: Please provide name of publisher for reference 13.	
Q6	AUTHOR: Please provide page number for reference 14.	
Q7	AUTHOR: Please provide name of publisher for reference 16.	
Q8	AUTHOR: Please provide publisher name for reference 24.	
Q9	AUTHOR: Please provide publisher name for reference 26.	
Q10	AUTHOR: Please provide name of publisher for reference 29.	

WILEY

USING e-ANNOTATION TOOLS FOR ELECTRONIC PROOF CORRECTION

Required software to e-Annotate PDFs: <u>Adobe Acrobat Professional</u> or <u>Adobe Reader</u> (version 7.0 or above). (Note that this document uses screenshots from <u>Adobe Reader X</u>)
The latest version of Acrobat Reader can be downloaded for free at: <u>http://get.adobe.com/uk/reader/</u>

Once you have Acrobat Reader open on your computer, click on the Comment tab at the right of the toolbar:
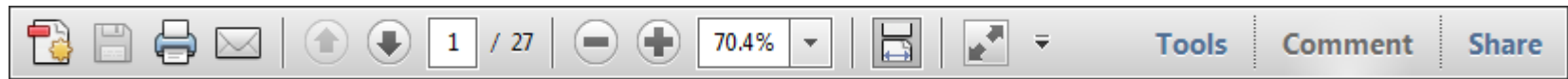
This will open up a panel down the right side of the document. The majority of tools you will use for annotating your proof will be in the Annotations section, pictured opposite. We've picked out some of these tools below:

---
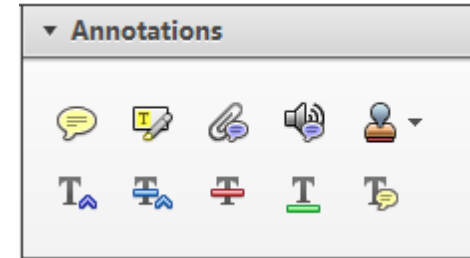
1. Replace (Ins) Tool – for replacing text.

Strikes a line through text and opens up a text box where replacement text can be entered.

How to use it

- Highlight a word or sentence.
- Click on the Replace (Ins) icon in the Annotations section.
- Type the replacement text into the blue box that appears.

---
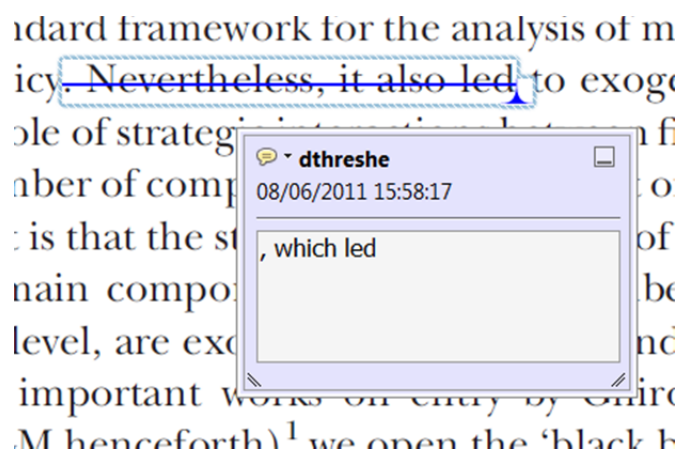
2. Strikethrough (Del) Tool – for deleting text.

Strikes a red line through text that is to be deleted.

How to use it

- Highlight a word or sentence.
- Click on the Strikethrough (Del) icon in the Annotations section.

---
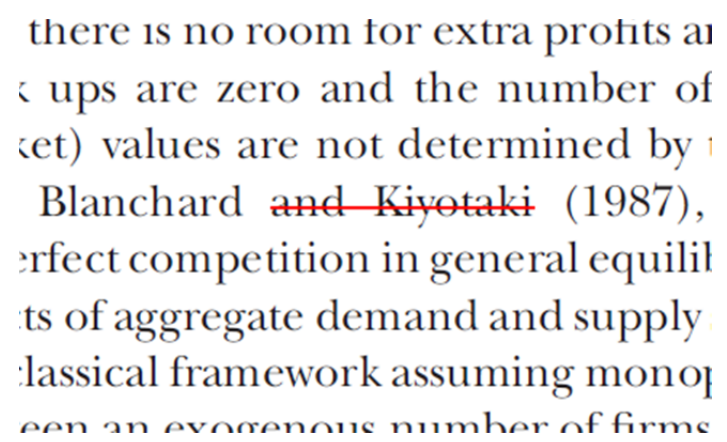
3. Add note to text Tool – for highlighting a section to be changed to bold or italic.

Highlights text in yellow and opens up a text box where comments can be entered.

How to use it

- Highlight the relevant section of text.
- Click on the Add note to text icon in the Annotations section.
- Type instruction on what should be changed regarding the text into the yellow box that appears.
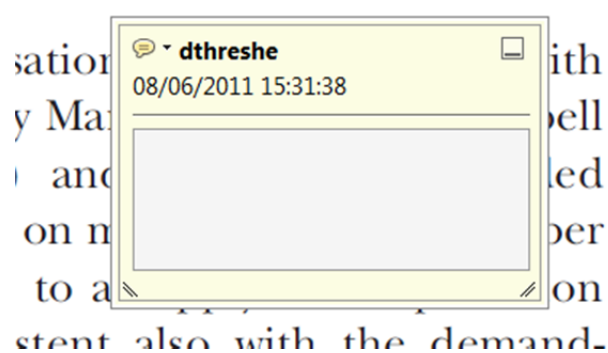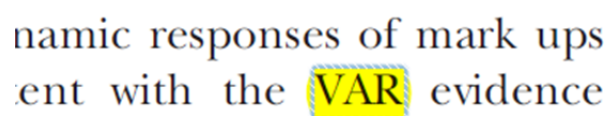
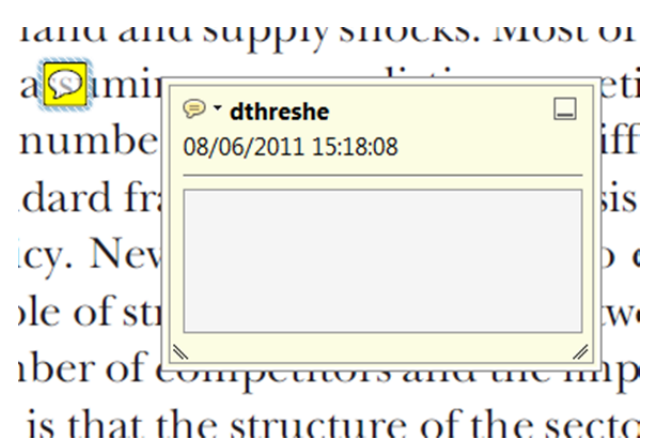
4. Add sticky note Tool – for making notes at specific points in the text.

Marks a point in the proof where a comment needs to be highlighted.

How to use it

- Click on the Add sticky note icon in the Annotations section.
- Click at the point in the proof where the comment should be inserted.
- Type the comment into the yellow box that appears.

5. Attach File Tool – for inserting large amounts of text or replacement figures.

Inserts an icon linking to the attached file in the appropriate pace in the text.

How to use it

- Click on the Attach File icon in the Annotations section.
- Click on the proof to where you'd like the attached file to be linked.
- Select the file to be attached from your computer or network.
- Select the colour and type of icon that will appear in the proof. Click OK.
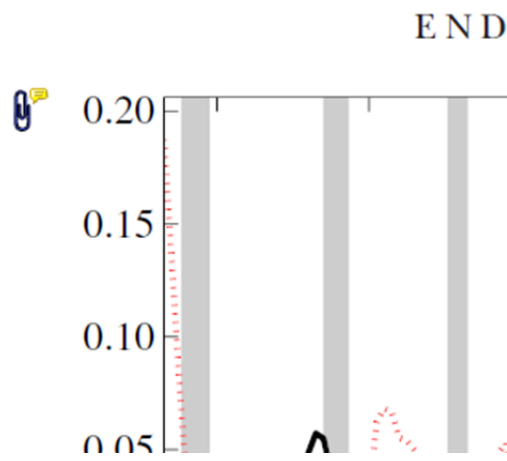
6. Add stamp Tool – for approving a proof if no corrections are required.

Inserts a selected stamp onto an appropriate place in the proof.

How to use it

- Click on the Add stamp icon in the Annotations section.
- Select the stamp you want to use. (The Approved stamp is usually available directly in the menu that appears).
- Click on the proof where you'd like the stamp to appear. (Where a proof is to be approved as it is, this would normally be on the first page).

7. Drawing Markups Tools – for drawing shapes, lines and freeform annotations on proofs and commenting on these marks.

Allows shapes, lines and freeform annotations to be drawn on proofs and for comment to be made on these marks..

How to use it

- Click on one of the shapes in the Drawing Markups section.
- Click on the proof at the relevant point and draw the selected shape with the cursor.
- To add a comment to the drawn shape, move the cursor over the shape until an arrowhead appears.
- Double click on the shape and type any text in the red box that appears.
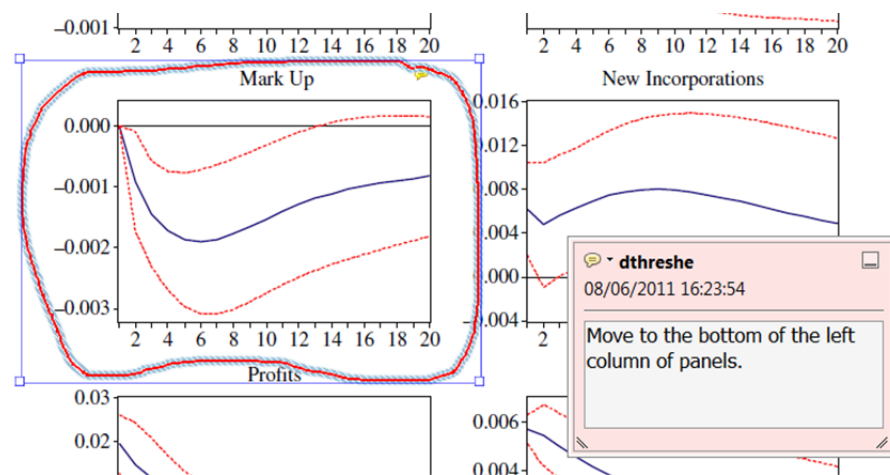
For further information on how to annotate proofs, click on the Help menu to reveal a list of further options: